Available online at www.sciencedirect.com
SCIENCE DIRECT®

Journal of the European Ceramic Society 25 (2005) 1067–1072

www.elsevier.com/locate/jeurceramsoc

Reaction sintering of AlN–AlON composites

A. Maghsoudipour[a,*], M. A. Bahrevar[a], J. G. Heinrich[b], F. Moztarzadeh[a]

[a] *Materials and Energy Research Center, PO Box 14155-4777, Tehran, Iran*
[b] *Institute of Non Metallic Materials, Technical University Clausthal, Clausthal-Zellerfeld, Germany*

Received 25 September 2003; received in revised form 29 March 2004; accepted 20 April 2004
Available online 15 July 2004

Abstract

Sintering behavior of three different compositions in the AlN–Al_2O_3 system using Y_2O_3 as a sintering aid was investigated. Samples with various ratios of AlN/Al_2O_3 were sintered in nitrogen atmosphere using a gas pressure furnace in the temperature range 1750–1950 °C. The densification of the samples was studied by shrinkage and relative density measurements. Results showed that samples containing 1 and 70 wt.% alumina were sintered to near theoretical density at 1800 °C; whereas the sample with 20 wt.% alumina never reached densities higher than 93% in the temperature range considered. It was found that the AlN/Al_2O_3 ratio and the sintering temperature had a great influence on the microstructure and crystalline phases present in the samples, namely, AlN, γ-AlON, 27R, and YAG. In the sample with 20 wt.% alumina, porosity formation prevented further densification. These porosities were probably due to the release of oxygen during sintering.

Keywords: Nitrides; Composites; Sintering; Functional application; Oxynitrides; AlN; AlON

1. Introduction

Aluminum nitride ceramics are noted for their excellent thermal properties, high-temperature mechanical properties, low dielectric constant, and thermal expansion coefficients. There is a wealth of literature[1–3] on the processing and properties of this material. However, like other non-oxide ceramics, their low resistance to oxidation and high sintering temperature required for densification are considered disadvantages which renders them unsuitable for certain applications.[4,5] In order to lower the sintering temperature and improve some of the properties, the role of different additives such as Y_2O_3, CaO, YF_3, and Al_2O_3 has been extensively studied.[6–10] Efforts have also been made to improve the oxidation resistance at the expense of thermal properties. Therefore, different compositions in the AlN–Al_2O_3 system have been studied.[11,12]

The addition of Al_2O_3 to AlN leads to the formation of aluminum oxynitride phases. Corbin[13] has listed thirteen different aluminum oxynitride phases which are separated into two groups according to their crystallographic structures, one group is based on the polytypes of wurtzite structure and the other is based on the spinel structure of which γ-AlON is the most notable due to its optical properties. The sintering behavior of composites in the AlN–Al_2O_3 system has been studied by different authors.[1,14] Kim et al.[1] fabricated composites in the AlN–Al_2O_3 system containing 5, 30, 50, and 64.3 mol% Al_2O_3 using gas pressure sintering in the temperature range 1650–1900 °C. Their results indicated that the densities of all the samples increased with the sintering temperature up to 1750 °C. Further increase in the sintering temperature above 1750 °C decreased the sintered bulk densities. They attributed this decrease to the possible partial evaporation of the liquid phase. Kim et al.,[14] studied a similar system and achieved full density at 1800 °C. They also observed a decrease in density with an increase in temperature above 1800 °C. However, they attributed the decrease in density to the grain morphology and decomposability of the γ-AlON compound in the products.

In the present work, three compositions with different AlN/Al_2O_3 ratios corresponding to certain areas of the phase equilibrium diagram for the AlN–Al_2O_3 binary system were chosen. Y_2O_3 additive was also used to pro-

---

[*] Corresponding author. Tel.:+98 261 6204131; fax: +98 21 8773352.
E-mail address: amir@atlantico-online.de (A. Maghsoudipour).

0955-2219/$ – see front matter. © 2004 Elsevier Ltd. All rights reserved.
doi:10.1016/j.jeurceramsoc.2004.04.018

mote sintering. The various samples were sintered in a gas pressure furnace in nitrogen atmosphere in the temperature range 1750–1950 °C. Various phases, such as; AlN, γ-AlON ($Al_{23}O_{27}N_5$), 27R ($Al_9O_3N_7$), and YAG ($Al_5O_{12}Y_3$) could be detected in the samples, depending on the composition and sintering temperature. The effect of AlN/Al_2O_3 ratio and sintering temperature on the densification and microstructure has been discussed.

2. Experimental procedure

2.1. Raw materials

Commercially available aluminum nitride powder (Grade C, H.C. Starck) was mixed with 1, 2, and 70 wt.% Al_2O_3 (CT3000 SC, Alcoa) and an amount of Y_2O_3 (Meldform Metals) corresponding to Y_2O_3/AlN ratio equal to 2 wt.%. The samples were classified as A, B, and C, respectively. The average particle size and specific surface area of AlN powder were in the ranges 2.2–2.7 μm and 2.4–2.8 m^2/g and those of Al_2O_3 powder were in the ranges 0.5–0.8 μm and 6.5–8.5 m^2/g. The average particle size of Y_2O_3 powder was 0.75 μm.

2.2. Preparation and sintering

Different powder batches were mixed and homogenized by ball milling in ethanol for 5 h in a polyethylene bottle with alumina balls. After drying, the powder cake was crushed in an agate mortar and passed through a 20 mesh sieve. The granules were initially formed into pellets in a die press and then isostatically pressed at 50 MPa.

The samples were then placed in a BN-coated graphite crucible, embedded in AlN powder, and sintered in nitrogen atmosphere for 1 h using a gas pressure furnace (KCE, Special Furnace Co.).

Samples were sintered at five different temperatures, 1750, 1800, 1850, 1900, and 1950 °C. The initial pressure of nitrogen gas at room temperature was set to 2 bars which increased with any subsequent increase in temperature.

2.3. Evaluation

The shrinkage of samples was determined by the measurement of the sample size. Bulk density was determined by the Archimedes method. Powder density was measured by a helium-gas pycnometer (Quantachrome Ultrapycnometer 1000 version 1.60), hence relative density was calculated by dividing the bulk density to the powder density. High-temperature dilatometry was performed in nitrogen atmosphere (BAHR Thermoanalyse GmbH 1991–1993). Phase analyses were carried out using Philips PW 1729 diffractometer. Micrographs of the fractured surfaces were obtained using scanning electron microscopy (SEM, Cam Scan CS4).

3. Results and discussion

Fig. 1 shows the radial shrinkage of the three samples, A, B, and C versus the sintering temperature. It is evident from the figure that the shrinkage in all the samples increases to a maximum at approximately 1800 °C. However, samples A and C show a constant shrinkage above this temperature up to 1950 °C, whereas sample B exhibits a drop in shrinkage in the same temperature range. Samples A and C have the highest and lowest values of shrinkage at 1800 °C, respectively. The dilatometry curve of Fig. 2a as compared with Fig. 2b and c, confirms the high shrinkage of sample A.

The dilatometry curve of sample C in Fig. 2c shows an expansion between 1677 and 1722 °C, which results in a lower shrinkage in sample C compared to A (Fig. 1). In order to further investigate this anomaly, two more samples, having the same composition as sample C, were prepared and sintered at 1570 and 1750 °C (temperatures below and above the expansion range). XRD patterns of these samples are presented in Fig. 3. The diffractogram in Fig. 3a shows the presence of Al_2O_3 and AlN phases at 1570 °C whereas; the one in Fig. 3b indicates the presence of γ-AlON and AlN phases in the sample at 1750 °C. Therefore, we concluded that the γ-AlON phase has not formed up to 1570 °C and the expansion observed in the dilatometry curve at about 1700 °C can be attributed to the formation of the γ-AlON phase.

γ-AlON is formed through the reaction of AlN with Al_2O_3[13,15] according to the following equation:

$$5AlN + 9Al_2O_3 \rightarrow Al_{23}O_{27}N_5$$

A simple calculation based upon the theoretical volume expansion of the product, the density (ρ), and the molar mass (M) of the components can be considered as follows:

$$\rho_{AlN} = \frac{M}{V_{mol(AlN)}} = 3.25\,g/cm^3 \Longrightarrow V_{mol(AlN)} = 12.62\,cm^3$$

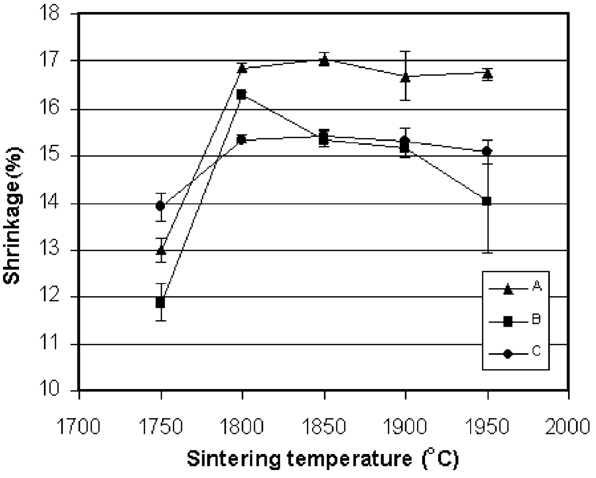

Fig. 1. Shrinkage of samples vs. sintering temperature.

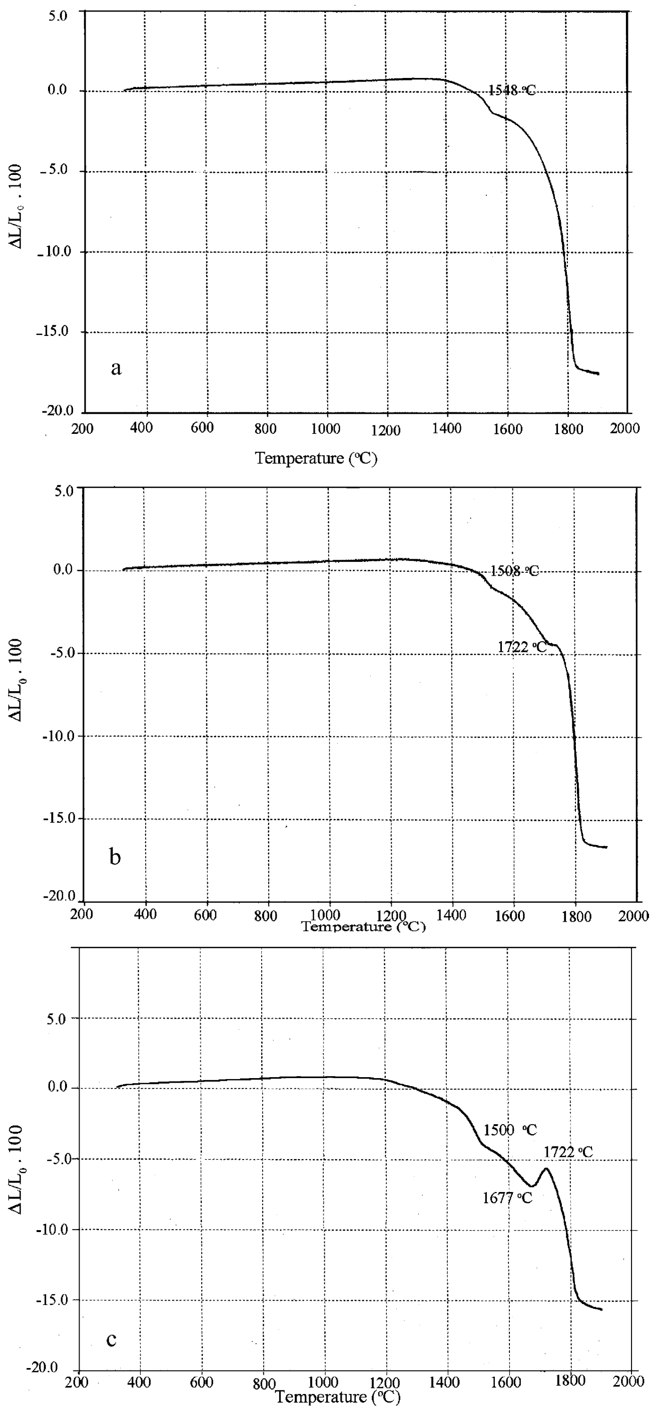

Fig. 2. Dilatometry curve of: (a) sample A, (b) sample B and (c) sample C.

$$\rho_{Al_2O_3} = \frac{M}{V_{mol(Al_2O_3)}} = 3.98\,g/cm^3 \Longrightarrow V_{mol(Al_2O_3)} = 25.63\,cm^3$$

$$\rho_{\gamma\text{-AlON}} = \frac{M}{V_{mol(\gamma\text{-AlON})}} = 3.72\,g/cm^3 \Longrightarrow V_{mol(\gamma\text{-AlON})} = 301.88\,cm^3$$

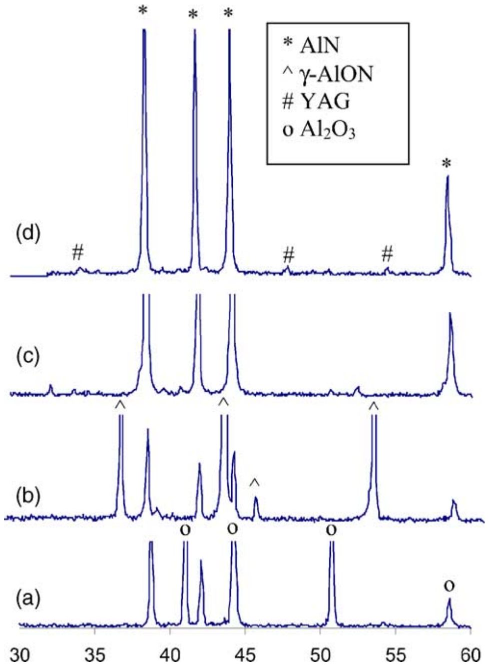

Fig. 3. XRD patterns of: (a) sample C sintered at 1570 °C, (b) sample C sintered at 1750 °C, (c) sample A sintered at 1500 and (d) sample A sintered at 1600 °C.

$$\left(\frac{\Delta V}{V}\right)\% = \left(\frac{V_{prod.} - V_{react.}}{V_{react.}}\right) \times 100 = 2.8\%$$

$$\frac{\Delta L}{L} = \frac{\Delta V/V}{3} = 0.9\%$$

The values of density and molar mass of AlN, Al_2O_3, and γ-AlON have been reported in different references.[16,17] It can be seen that the calculated linear expansion is quite close to the experimental value (1.1%) as determined by dilatometry in the temperature range 1677–1722 °C (Fig. 2c). This agreement indicates that the dilatometry technique can be

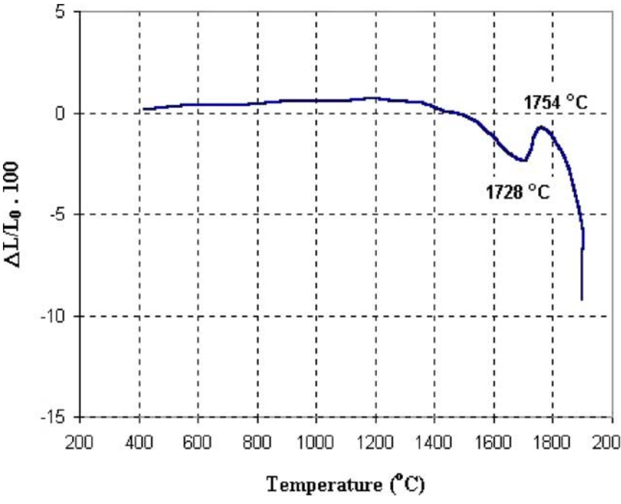

Fig. 4. Dilatometry curve of sample C without Y_2O_3.

efficiently used as an analytical tool in the evaluation of γ-AlON formation in the AlN–Al_2O_3 composite system.

Another feature observed in all three dilatometry curves (Fig. 2a–c) is the depression at temperatures 1548, 1508, and 1500 °C, respectively. In order to study the cause of this depression, different samples were prepared and fired at temperature below and above that of the depression. In case of composition A, XRD patterns of the two samples sintered at 1500 and 1600 °C are presented in Fig. 3c and d. It is seen that the predominant phase in Fig. 3c is AlN but in Fig. 3d both AlN and YAG ($Al_5O_{12}Y_3$) phases are present. Therefore, we can attribute the depression to the formation of the liquid phase, which on cooling precipitates YAG crystals. Furthermore, the addition of Y_2O_3 decreases the temperature of γ-AlON formation. Fig. 4 shows the dilatometry curve of sample C with no additive. It represents a lower shrinkage and a higher γ-AlON formation temperature (as compared with Fig. 2c). A similar behavior has been reported for MgO as a sintering additive.[15]

Sample B shows a different sintering behavior from that of the other two samples. As illustrated in Fig. 1, the sintering shrinkage decreases with increasing temperature above 1800 °C, which insinuates some kind of expansion at these temperatures. However, the dilatometry curve of sample B (Fig. 2b) does not support such a behavior and merely indicates a continuous shrinkage at these temperatures. It was, therefore, decided to investigate the microstructure of this sample sintered at different temperatures. The fracture sur-

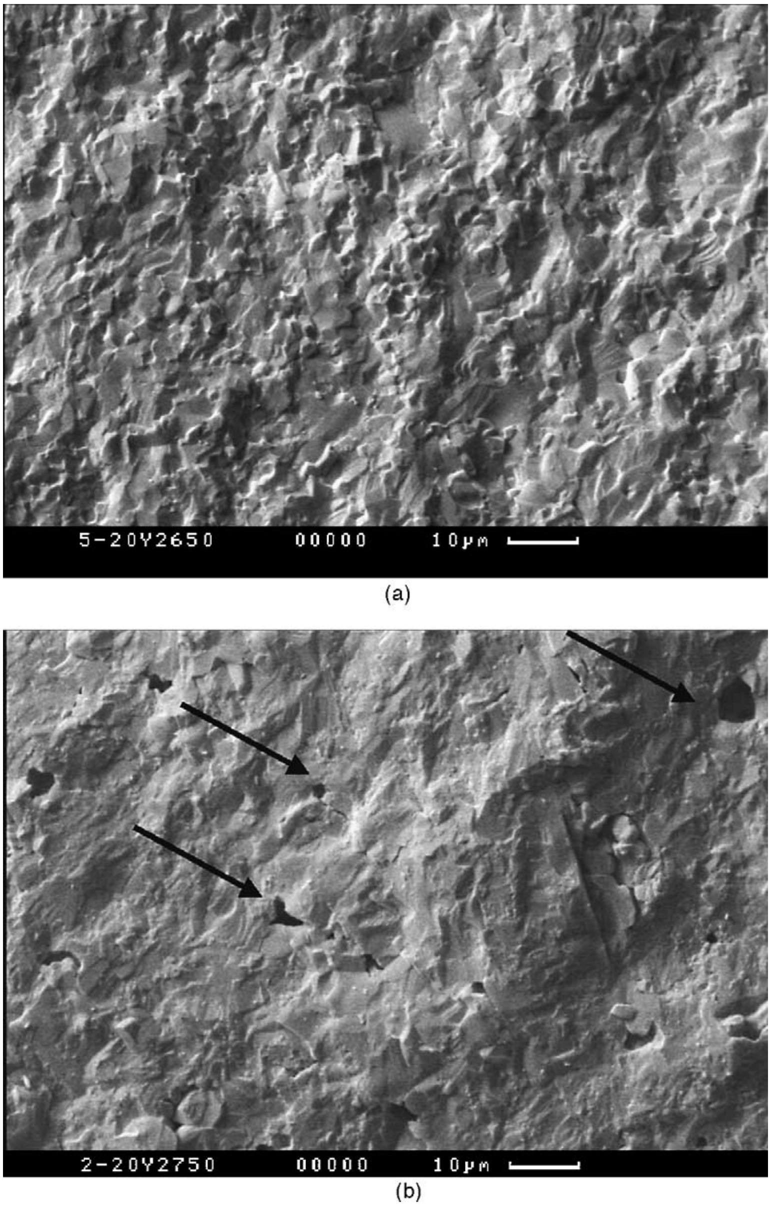

Fig. 5. SEM micrograph of fracture surface of the sample B sintered at: (a) 1800 °C and (b) 1900 °C.

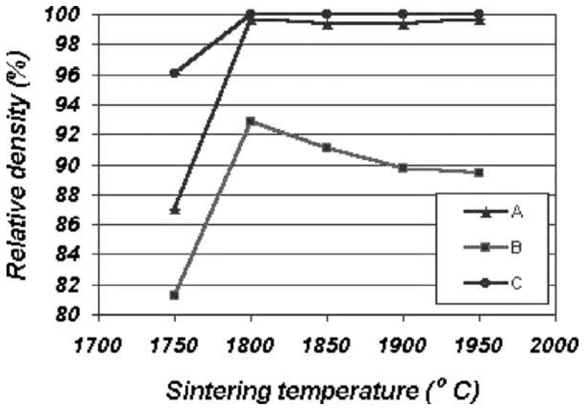

Fig. 6. Variation of relative density vs. sintering temperature.

face micrographs of B sintered at 1800 and 1900 °C are presented in Fig. 5a and b. The formation of porosities (illustrated by arrows) with increasing sintering temperature is obvious in Fig. 5b.

Further confirmation of porosity formation comes from measurements of relative density versus sintering temperature. Fig. 6 shows the variation of relative densities of the three samples with temperature up to 1950 °C. In case of sample B, the relative density increases up to 1800 °C and then falls off at higher temperatures. Fig. 7 shows the closed porosity of the three samples as a function of the sintering temperature. Close inspection of Figs. 6 and 7, indicates the presence of both open and closed pores in the samples up to about 1800 °C. Samples A and C exhibit near-theoretical density at and above this temperature. Fig. 7 indicates the elimination of open pores in sample B up to 1800 °C. It is also evident that closed porosity still exists; in fact, it is increased at higher temperatures.

A similar behavior has been observed and attributed to either the decomposition of γ-AlON phase[14] or partial evaporation of the liquid phase.[1] We have not been able to confirm either of these justifications in the present work. In spite of the high γ-AlON content in sample C and a substantial amount of liquid phase in sample A (due to its higher Y_2O_3 content), no such behavior has been observed and both have achieved near-theoretical density.

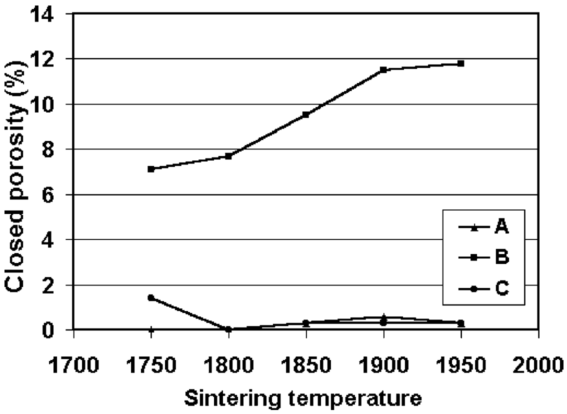

Fig. 7. Variations of closed porosity vs. sintering temperature.

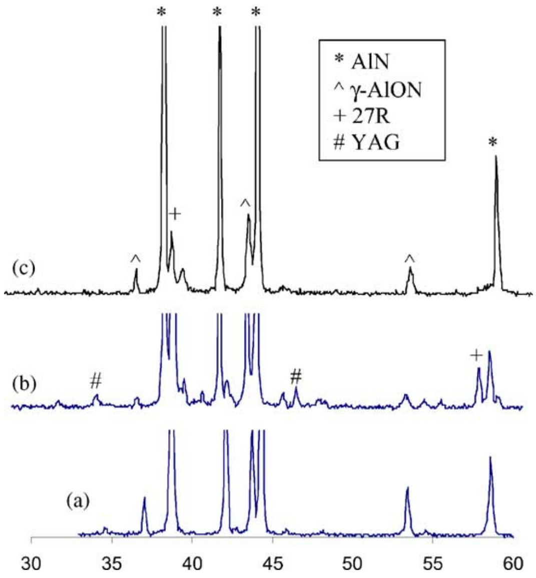

Fig. 8. XRD pattern of sample B sintered at: (a) 1800 °C in nitrogen atmosphere, (b) 1900 °C in nitrogen atmosphere and (c) 1900 °C in argon atmosphere.

Comparison of the X-ray diffraction pattern of samples B sintered at 1800 and 1900 °C shows the formation of the 27R phase at 1900 °C, in addition to AlN, γ-AlON and YAG phases common to both samples (Fig. 8a and b). Therefore, the 27R can be responsible for the formation of closed porosity.

According to the equilibrium phase diagram of the AlN–Al_2O_3 system,[13,18] the 27R polytype is formed at 1920 °C. In practice, the equilibrium conditions are not easily attainable and the reaction between γ-AlON and AlN is not fully accomplished. We, therefore, expect the initial components to manifest themselves in the X-ray pattern of Fig. 8b and, indeed, they do. The formation of the 27R phase is most probably the result of a reaction between AlN and γ-AlON. This reaction cold take place in several steps. A close investigation of the molar ratios of Al, N, and O, in the starting components (AlN and $Al_{23}O_{27}N_5$) and the reaction product; namely, the 27R phase ($Al_9O_3N_5$) indicates a demand for nitrogen and the evaluation of oxygen in the process. The evaluation of oxygen at these temperatures can be the cause of the porosity observed which inhibited further densification of the sample.

In order to confirm this point, two more samples with similar composition to sample B were sintered at 1800 °C to produce both AlN and γ-AlON phases. Both samples were then sintered at 1900 °C in separate atmospheres; namely, argon and nitrogen. The sample sintered in argon (Fig. 8c) shows a considerable drop in 27R phase as compared with Fig. 8b which supports our proposition. Therefore, it can be inferred that the closed pores are due to oxygen evaluation.

4. Conclusions

Samples with 1, 20, and 70 wt.% alumina were fabricated in the AlN–Al_2O_3 system, using Y_2O_3 as a sintering aid. Samples with 1 and 70 wt.% alumina were sintered to near-theoretical density at 1800 °C. Phase analysis indicated the presence of AlN, γ-AlON and YAG in these samples. However, the YAG content in the sample with 70 wt.% alumina was negligible. The dilatometry technique could well be employed to investigate the formation temperature of γ-AlON in this system.

The maximum relative density achieved for the sample with 20 wt.% alumina, was 93% at 1800 °C. AlN, γ-AlON, and YAG were the only high-temperature phases detected up to 1800 °C. Above this temperature, the 27R phase was also observed. We conclude that the formation of 27R phase is the result of the reaction between AlN and γ-AlON in nitrogen atmosphere with the result of the reaction of oxygen in the process. This may be the cause of closed pores which inhibit further densification.

Acknowledgements

The first author would like to thank Materials and Energy Research Center (Iran) and Technical University Clausthal (Germany) for the economical and experimental support extended to him.

References

1. Kim, Y. W., Park, B. H., Lee, Y. B., Oh, K. D. and Riley, F. L., Sintering, microstructure, and mechanical properties of AlON–AlN particulate composites. *Br. Ceram. Trans.* 1998, **97**, 97–104.
2. Watari, K., Ishizaki, K. and Fujikawa, T., Thermal conduction mechanism of aluminum nitride ceramics. *J. Mater. Sci.* 1992, **27**, 2627–2630.
3. Watari, K., Ishizaki, K. and Tsuchiya, F., Phonon scattering and thermal conduction mechanisms of sintered aluminum nitride ceramics. *J. Mater. Sci.* 1993, **28**, 3709–3714.
4. Abid, A., Bensalem, R. and Sealy, B. J., The thermal stability of AlN. *J. Mater. Sci.* 1986, **21**, 1301–1304.
5. Barthelme, P., Ansorge, F., Kulig, M., Hofmann, T. and Russel, C., The sintering and oxidation behavior of aluminum nitride. *J. Eur. Ceram. Soc.* 1989, **1**, 1.479–1.483.
6. Hundere, M. and Einarsrud, M. A., Effects of reduction of the Al–Y–O containing secondary phases during sintering of AlN with YF_3 additions. *J. Eur. Ceram. Soc.* 1996, **16**, 899–906.
7. Hundere, A. M. and Einarsrud, M. A., Microstructure development in AlN(YF_3) ceramics. *J. Eur. Ceram. Soc.* 1997, **17**, 873–878.
8. Neumann, N., Reetz, T. and Rucssel, C., The influence of the anions of calcium-containing sintering aids for aluminum nitride. *J. Eur. Ceram. Soc.* 1993, **12**, 117–122.
9. Inoue, K. H. and Tsuge, A., Effect of various additives on sintering of aluminum nitride. *Yogyo Kyokai Shi.* 1981, **89**, S94–S100.
10. Hirano, M., Kato, K., Isobe, T. and Hirano, T., Sintering and characterization of fully dense aluminum nitride ceramics. *J. Mater. Sci.* 1993, **28**, 4725–4730.
11. Fievez, F., Goeuriot, P. and Thevenot, F., Oxidation kinetics of alumina–γ-aluminum oxynitride composites with Y_2O_3 or MgO sintering additives. In *High Temperature Corrosion of Technical Ceramics*, ed. R. J. Fordham. Elsevier Applied Science, London.
12. Quinn, G. D., Corbin, N. D. and McCauley, J. W., Thermomechanical properties of aluminum oxynitride spinel. *Am. Ceram. Soc. Bull.* 1984, **63**, 723–730.
13. Corbin, N. D., Aluminum oxynitride spinel: a review. *J. Eur. Ceram. Soc.* 1989, **5**, 143–154.
14. Kim, N. H., Fun, Q. D., Komeya, K. and Meguro, T., Phase reaction and sintering behavior in the pseudoternary system AlN–Y_2O_3–Al_2O_3. *J. Am. Ceram. Soc.* 1996, **79**, 2645–2651.
15. Yawei, L., Nan, L. and Runzhang, Y., The formatin and stability of γ-aluminum nitride spinel in the carbothermal reduction and reaction sintering processes. *J. Mater. Sci.* 1997, **32**, 979–982.
16. Schneider, S. J., *Engineered Materials Handbook (Vol. 4)—Ceramics and Glasses*. ASM International, 1991, p. 191.
17. Hirano, M. and Yamauchi, N., Development of as-fired aluminum nitride substrates with smooth surface and high thermal conductivity. *J. Mater. Sci.* 1993, **28**, 5737–5743.
18. McCauley, J. W. and Corbin, N. D., High temperature reactions and microstructure in the Al_2O_3–AlN system. In *Progress in Nitrogen Ceramics*, ed. F. L. Riley. Martinus Nijhoff Publishers, Boston, 1983, pp. 111–118.